Research Square

Preprints are preliminary reports that have not undergone peer review.
They should not be considered conclusive, used to inform clinical practice,
or referenced by the media as validated information.

Corrosion Inhibition of Stainless Steel Grade 202 by Combined Coatings of Banana Peel Powder, Polyaniline and CuO in Hydrochloric Acid Medium

P. O. Alliyadde
University of Peradeniya
N. Priyantha
namal.priyantha@yahoo.com
University of Peradeniya

Research Article

Keywords:

Posted Date: November 9th, 2026

DOI: https://doi.org/10.21203/rs.3.rs-11591157/v1

License: This work is licensed under a Creative Commons Attribution 4.0 International License.
Read Full License

Additional Declarations: No competing interests reported.

Corrosion Inhibition of Stainless Steel Grade 202 by Combined Coatings of Banana Peel Powder, Polyaniline and CuO in Hydrochloric Acid Medium

P.O. Alliyadde[1], N. Priyantha[2*]

[1]*Department of Environmental and Industrial Sciences, University of Peradeniya, Peradeniya, Sri Lanka.*
[2]*Department of chemistry, University of Peradeniya, Peradeniya, Sri Lanka*

***Corresponding author:** Namal Priyantha, Department of Chemistry, University of Peradeniya, Peradeniya, Sri Lanka, 20400

P.O. Alliyadde
E-mail address: priyanjalaomali@gmail.com

N. Priyantha
E-mail address: namal.priyantha@yahoo.com

Corrosion Inhibition of Stainless Steel Grade 202 by Combined Coatings of Banana Peel Powder, Polyaniline and CuO in Hydrochloric Acid Medium

Abstract

Corrosion of steel in acidic media remains a major challenge in industrial applications, particularly for cost-effective alloys such as Stainless Steel (SS) Grade 202. This study aims to develop an environmentally friendly, low-cost, and efficient corrosion-inhibition system using banana peel powder (BPP) extract, polyaniline (PANI) and copper oxide (CuO), tested individually and in synergistic combinations. The BPP extract prepared through refluxing to isolate bioactive phytochemicals is responsible for adsorption on the SS surface. Moreover, CuO particles synthesized using chemical (sol-gel) and green synthesis methods, when combined with carbonized BPP, overcomes the degradation issue of BPP alone, demonstrating strong corrosion inhibitory activity of SS Grade 202 in 0.50 mol L^{-1} HCl medium, as evidenced by mass loss measurements, open circuit potential measurements, electrochemical impedance spectroscopy and Tafel polarization. More importantly, BPP+PANI+CuO combined coating exhibits superior corrosion inhibitory performance, reflected by enhanced charge-transfer resistance, reduced corrosion current density, and more noble corrosion potential values. Scanning electron microscopic analysis confirms improved surface coverage and reduced pitting of the combined coating. Overall, synergistic interactions among BPP, PANI and CuO significantly enhances corrosion resistance of SS Grade 202 in HCl environments.

Keywords: Banana peel powder (BPP), combined coating, CuO, corrosion inhibition, polyaniline

1.Introduction

Stainless steels play a critical role in chemical processing, construction, transportation, and energy-related industries due to their favorable mechanical properties, strong formability, and relatively high resistance to corrosion [1]. Among various grades, austenitic stainless steel (SS) Grade 202 has gained widespread attention, particularly in developing countries, as a cost-effective alternative to conventional nickel-rich stainless steels such as SS Grade 304 [2]. The reduced nickel content of SS Grade 202 lowers material cost, yet maintaining acceptable mechanical performance. However, this compositional modification results in diminished corrosion resistance, especially under aggressive conditions [3]. As a consequence, SS Grade 202 is vulnerable to corrosion in acidic environments, especially in the presence of chloride ions, which serve as a pitting agent [4].

Hydrochloric acid is extensively employed in industrial operations, such as pickling, descaling and acid cleaning [5]. In such environments, stainless steel surfaces are exposed to highly corrosive conditions that would lead to severe corrosion [6]. Chloride ions further aggravate this degradation by destabilizing the passive film on the steel surface, making corrosion mitigation a persistent challenge for SS Grade 202 in acidic media [7]. Traditionally, corrosion protection in acidic environments has relied on inorganic inhibitors and chromate-based coatings [8]. Although effective, these conventional systems are associated with significant drawbacks, including toxicity, poor biodegradability, and adverse environmental and health impacts [9]. Growing environmental awareness and increasingly strict regulatory frameworks have therefore accelerated the shift toward sustainable and environmentally benign corrosion inhibition strategies [10]. In this context, green corrosion inhibitors derived from plant materials, biomass, and agricultural waste have emerged as promising alternatives due to their renewability, low toxicity, biodegradability and economic viability [11, 12].

Among various biomass-based materials, banana peel waste represents an attractive green inhibitor source [13]. Banana peels are commonly discarded without value addition, and they are rich in cellulose, hemicellulose, lignin, pectin, proteins and diverse phytochemical constituents, such as polyphenols, flavonoids and tannins [14,15]. These components contain electronegative functional groups such as hydroxyl, carboxyl and amine moieties, which can interact strongly

with metal surfaces through physical and chemical adsorption mechanisms [16]. Such interactions facilitate the formation of protective surface films reducing metal dissolution in acidic environments [17]. Despite their promising corrosion inhibition performance, banana peel-based inhibitors often suffer from poor film stability, leaching of active components, and limited long-term effectiveness when applied alone [18].

To address stability limitations of biomass-derived inhibitors, conductive polymers have been increasingly explored as corrosion-protective coatings [19]. Polyaniline (PANI), in particular, has attracted significant attention due to its unique redox behavior, environmental stability, ease of synthesis, and ability to induce passivation on metallic substrates [20]. Electrochemically deposited PANI coatings would serve as physical barriers while simultaneously stabilizing the metal surface through redox-mediated passivation processes [21]. Furthermore, electrochemical polymerization enables precise control over coating thickness, morphology, and adhesion [22]. Nevertheless, PANI coatings alone may contain microstructural defects and inherent porosity, allowing electrolyte penetration and reducing their effectiveness in strongly acidic environments [23]. As a constructive step forward, recent research has focused on combined coating strategies that integrate inorganic fillers or particles within polymer-based matrices to further enhance corrosion resistance [24]. Metal oxide particles such as TiO_2, ZnO, and CuO have been reported to improve coating compactness, decrease permeability, and strengthen protective layers by blocking defect pathways [25]. Among these, CuO particles are of particular interest due to their chemical stability, semiconducting nature, and strong interfacial interactions with both polymer matrices and metal substrates [26]. The incorporation of CuO particles would therefore improve both the protective efficiency and durability of polymer-based coatings [27].

Despite these advances, studies that systematically combine agro-waste-derived green inhibitors with electrochemically deposited conductive polymers and inorganic oxide particles for the corrosion protection of SS Grade 202 in acidic environments remain scarce [28]. In particular, limited attention has been given to addressing the long-term stability issues of biomass-based inhibitors through rational combined coating design [29]. In this context, the present study investigates the corrosion inhibition performance of combined coatings based on banana peel powder (BPP), PANI and CuO particles on SS Grade 202 in HCl medium [30, 31]. A comprehensive range of coating configurations, including individual coatings, binary

combinations, and a ternary combined coating, was evaluated to elucidate synergistic effects among the coating components [32]. Special emphasis was placed on improving the long-term stability of banana peel-based coatings through the incorporation of CuO particles [33]. Corrosion behavior was assessed using gravimetric measurements, open circuit potential (OCP) monitoring, potentiodynamic polarization, and electrochemical impedance spectroscopy (EIS) [34,35]. The outcomes of this study provide mechanistic insight into the synergistic corrosion inhibition behavior of combined coatings and demonstrate a sustainable, agro-waste-based strategy for enhancing the corrosion resistance of SS Grade 202 in acidic environments [36].

2. Materials and Methods

2.1 Materials

SS Grade 202 was used as the substrate material. The nominal chemical composition of SS Grade 202 is presented in Table 1. Banana peels ('Amban' variety in Sinhala) were collected from local sources and processed into powder, and the extract was prepared as described in Section 2.3 [13, 37]. Oxalic acid, copper (II) sulfate pentahydrate ($CuSO_4 \cdot 5H_2O$), citric acid, and hydrochloric acid used in this study were of analytical grade. Distilled water was used for all solution preparations.

Table 1: Chemical composition of SS Grade 202 (%).

SS Grade 202	C	Mn	P	S	Si	Cr	Ni	Fe	N
	≤ 0.15	7.50-10.00	≤ 0.06	≤ 0.03	≤ 1.00	17.0-19.0	4.0-6.0	≤ 68.0	≤ 0.25

2.2 Instrumentation

Fourier transform infrared (FTIR) spectra of banana peel powder (BPP) before and after reflux extraction were recorded using an IRPrestige-21 FTIR spectrometer (Shimadzu Corporation, Japan). The elemental composition of the synthesized copper oxide (CuO) particles was analyzed using an X-ray fluorescence (XRF) spectrometer (Fischerscope, Model DF500FG-456), while

their crystalline structure was characterized using an X-ray diffractometer (Ultima IV, Rigaku Corporation, Japan). The surface morphology of the coated stainless steel (SS) Grade 202 specimens was examined using a scanning electron microscope (EVO LS15, Carl Zeiss, Germany). Thermogravimetric analysis (TGA) of raw BPP, synthesized CuO, and the carbonized BPP–CuO composite was performed using a simultaneous thermal analyzer (SDT Q600, TA Instruments, USA). Mass measurements were carried out using an analytical balance (Model AA 220/C/2).

Electrochemical polymerization, electrochemical impedance spectroscopy (EIS), and potentiodynamic polarization measurements were performed using a potentiostat/galvanostat (PGSTAT204, Metrohm Autolab, The Netherlands). Electrochemical data were analyzed using NOVA software (version 2.1.7). A three-electrode configuration consisting of an SS Grade 202 working electrode, a platinum counter electrode, and an Ag/AgCl reference electrode was employed. Open-circuit potential (OCP) measurements were recorded using a digital multimeter (GDM-8145).

2.3 Preparation of BPP Extract

Dried banana peels were pulverized into a fine powder. Weighed mass of 10.000 g was subjected to reflux extraction in 170 mL deionized water at 80 °C for 2.0 h [37]. The mixture was filtered to obtain a clear supernatant, which served as the BPP inhibitor extract [38].

2.4 Preparation of CuO (Chemical Synthesis)

A sample of 2.500 g of $CuSO_4 \cdot 5H_2O$ was dissolved in 50.00 mL of distilled water. Citric acid (1.920 g) was added and the mixture was stirred at 85 °C until a thick gel was formed [39]. The gel was dried at 110 °C for 48 h and calcined at 800 °C for 3.0 h to obtain CuO powder [40].

2.4.1 Preparation of CuO (Green Synthesis)

Particles of CuO were also synthesized via a green route using the plant extract as a reducing and stabilizing agent [41]. Solution of $CuSO_4 \cdot 5H_2O$ was allowed to react with the extract under heating and continuous stirring. The resulting precipitate was collected by filtration, washed repeatedly, and oven-dried [42].

2.5 Preparation of PANI Coatings

PANI was electrodeposited potentiodynamically from aqueous solution containing 0.30 mol L^{-1} oxalic acid and 0.10 mol L^{-1} aniline [43]. Cyclic voltammetry was performed over a potential window of –0.2 V to +1.4 V vs. Ag/AgCl at a scan rate of 10 mV s^{-1} for 450 cycles to achieve a uniform, adherent coating [44].

2.6 Preparation of Combined Coatings

Combined coatings were developed by incorporating BPP, CuO particles, and electrochemically deposited PANI in different combinations to systematically evaluate individual, binary, and ternary corrosion inhibition effects on SS Grade 202 [28]. For combined coatings involving PANI, an optimized amount of BPP extract and a predetermined mass of CuO particles were introduced into the aniline–oxalic acid electrolyte prior to electropolymerization [27]. Electrodeposition was then carried out under identical potentiostatic conditions, resulting in PANI-based combined coatings with embedded BPP-derived phytochemicals and CuO particles [27]. Initially, corrosion performance was evaluated for the following coating systems: (a) uncoated SS Grade 202 (blank), (b) BPP-coated, (c) CuO-coated, (d) PANI-coated, (e) BPP+CuO combined coating, (f) CuO+PANI combined coating, (g) BPP+PANI combined coating, and (h) BPP+CuO+PANI combined coating [32]. This systematic approach enabled clear differentiation of the protective contributions of each component and the assessment of possible synergistic interactions [33]. Particular attention was given to the BPP+CuO combined coating to address the long-term stability limitations commonly associated with biomass-based inhibitors; the incorporation of CuO particles was intended to reinforce the BPP-derived protective layer, reduce leaching of active organic constituents, and enhance coating durability under acidic conditions [33]. All coatings were applied onto SS Grade 202 substrates under controlled and reproducible conditions, and the coated specimens were allowed to stabilize prior to gravimetric and electrochemical corrosion measurements [34].

2.7 Surface Preparation of SS 202 Specimens

SS 202 specimens were cleaned with distilled water, degreased with acetone, and dried prior to coating deposition and corrosion testing [35].

2.8 Method of Analysis

2.8.1 Mass loss method

The mass loss method, a simple and widely accepted gravimetric technique, was employed to evaluate corrosion rates and inhibition performance [45]. Pre-weighed metal specimens were immersed in the corrosive medium for a fixed exposure period (typically 24 h) at controlled temperature [46]. After immersion, the samples were cleaned, dried, and re-weighed. The percentage mass loss was calculated using Eq. (1), and inhibition efficiency was determined from the reduction in mass loss relative to the uninhibited system using Eq. (2) [47]. All experiments were performed in triplicate, and results are reported as mean values with standard deviations [48].

$$\text{Mass loss percentage} = \left(\frac{m_0 - m}{m_0}\right) \times 100\% \qquad (1)$$

$$\text{Inhibition efficiency (\%)} = \left(\frac{m}{m_0}\right) \times 100\% \qquad (2)$$

where m_0 and m represent the initial and final masses of the metal specimen, respectively [49].

2.8.2 Electrochemical measurements

EIS measurements were conducted over a frequency range of 0.1 Hz to 1 MHz with a 10 mV RMS sinusoidal perturbation [50]. Potentiodynamic polarization scans were performed from –0.1 V to +0.1 V vs. OCP at a scan rate of 0.01 mV s^{-1} [51]. Data were analyzed using equivalent circuit modeling and Tafel extrapolation [52].

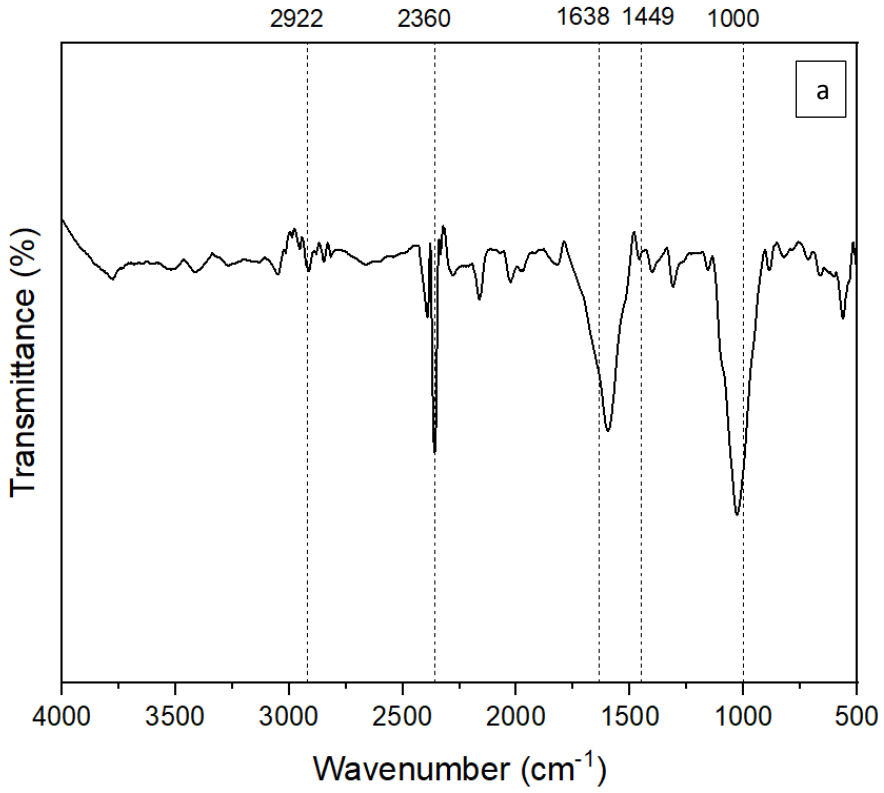
2.8.3 Open circuit potential (OCP) measurement

OCP was measured versus a saturated Ag/AgCl reference electrode [53]. The measurement protocol comprised frequent sampling during the initial 10 h (every 10 minutes for the first hour, then every 2 h) followed by daily measurements for up to 15 days [54].

3. Results and Discussion

3.1 Characterization of BPP Before and After Refluxing Using FTIR

Figure 1 shows that the FTIR spectrum of BPP before refluxing contains the characteristic C–H, C≡C, C=O, aromatic C–H, and C–O peaks typical of raw banana peel [15]. After refluxing, both the liquid extract and the solid residue also exhibit the same set of major peaks, with only minor differences in intensity [16]. This confirms that the refluxing process did not generate new functional groups or alter the chemical structure of BPP; it simply separated the same inherent compounds between the liquid and solid fraction [17].



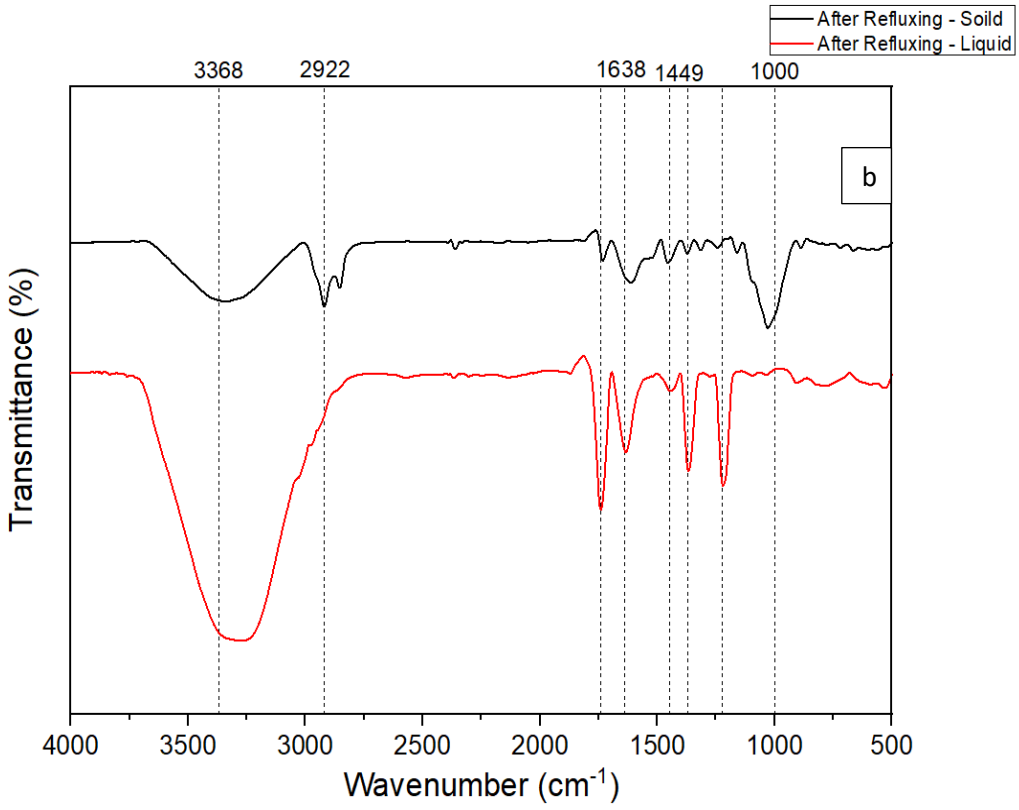


Figure 1: FTIR spectrum of BPP (a) before refluxing (b) after refluxing.

3.1.1 Phytochemical screening tests for BPP extract

Phytochemical screening tests conducted on the refluxed BPP extract to identify the presence of bioactive compounds responsible for corrosion inhibition confirmed the existence of polyphenols, flavonoids, and tannins, which are known to adsorb onto metal surfaces and form protective layers (Table 2) [18,19].

Table 2: Results of phytochemical screening tests conducted on BPP extract [19].

Phytochemical Class	Test Conducted	Observation	Result
Polyphenols	Ferric chloride ($FeCl_3$) spot test	Dark green solution with precipitate	Positive (+)
Flavonoids	NaOH alkaline test	Intense orange solution	Positive (+)
Tannins	Lead acetate [$Pb(CH_3COO)_2$] test	Yellowish precipitate	Positive (+)

Preliminary phytochemical tests confirmed the presence of key inhibitory compounds in the BPP extract: polyphenols (dark green $FeCl_3$ test), flavonoids (orange NaOH test), and tannins (yellowish lead acetate precipitate) [55]. These bioactive groups are well known for adsorption, chelation, and protective film formation, collectively supporting the extract's potential as an effective green corrosion inhibitor [56].

3.2 Characterization of CuO using XRF

XRF is a technique used to detect the elemental composition of a sample by investigating the characteristic X-rays emitted when the sample is bombarded with high-energy radiation [57]. XRF spectrum recorded for synthesized CuO particles clearly shows a highly intense peak for Cu with a minor peak for Fe (Figure 2). Peak intensities being analogous to the concentration of each element indicate that Fe is a trace, which may be due to impurities [58,59].

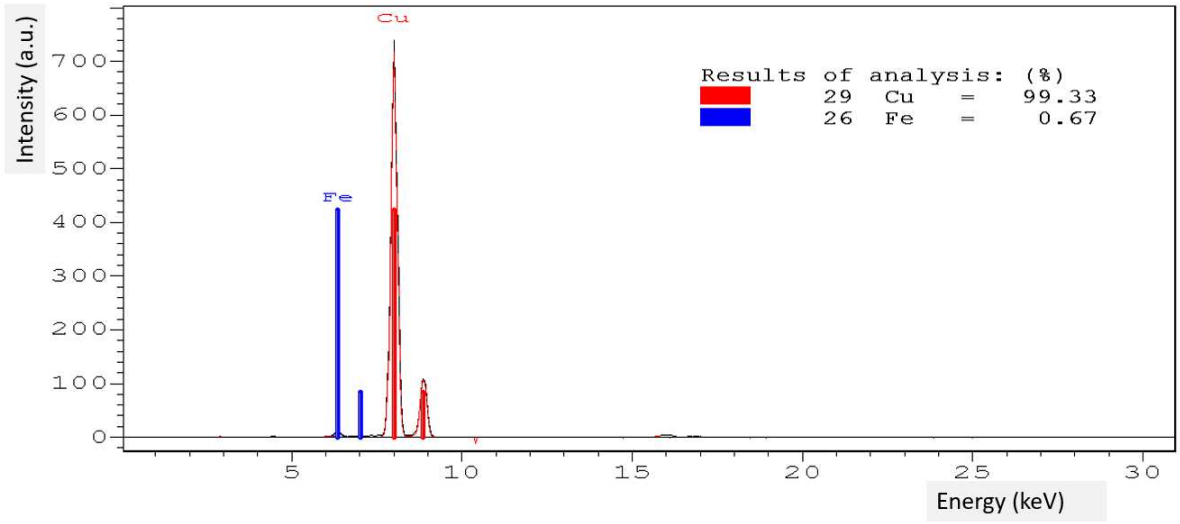


Figure 2: XRF of synthesized CuO.

3.2.1 Characterization of CuO using XRD

XRD analysis provides information on the crystalline structure and the crystallite size of material [60]. The XRD pattern, given in Figure 3, shows distinct diffraction peaks characteristic of monoclinic CuO, with major reflections at 35.5°, 38.7°, and 48.8°, corresponding to the (002), (111) and (202) planes, respectively [39]. These peaks match the standard reference pattern

(JCPDS 45-0937), confirming that the material is phase-pure CuO with no detectable impurities [40]. Crystallite sizes calculated using the Scherrer equation, which relates peak broadening (FWHM), Bragg angle (θ), X-ray wavelength (λ = 0.154 nm) and the shape factor (K = 0.94), are shown in Table 3 [41]. The average crystallite size of 14.3 nm indicates that CuO possesses a fine crystalline domain size [42]. Such smaller crystallites are advantageous for corrosion-related applications, as they enhance surface area, dispersion, and interfacial interaction within composite systems [43].

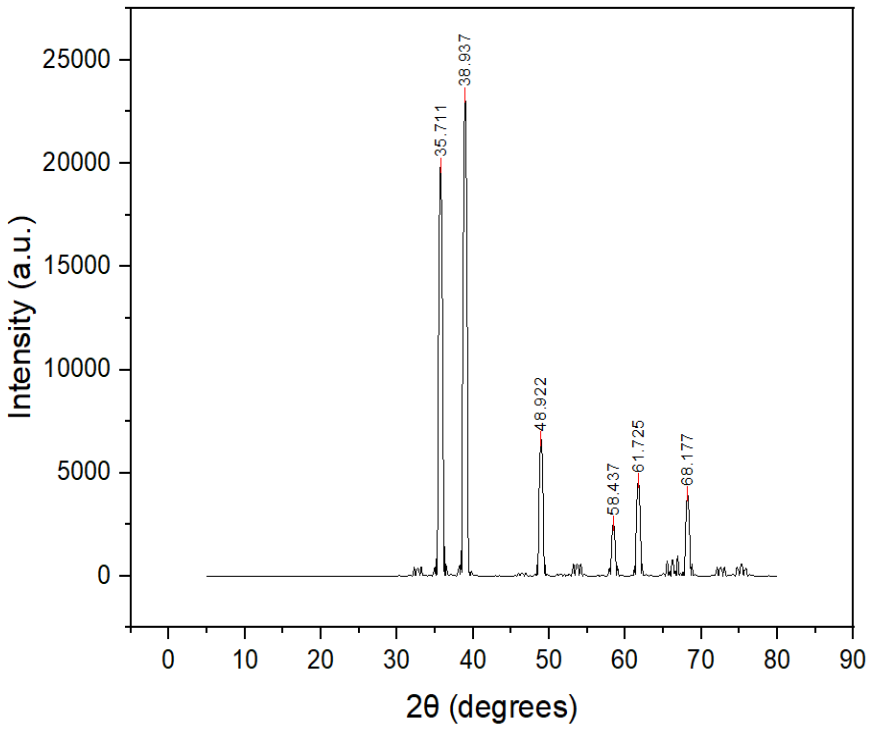


Figure 3: X-ray diffraction pattern of synthesized CuO particles.

Table 3: Crystallite size calculation for CuO from XRD data [41].

2θ (°)	**FWHM (radians)**	**Crystallite size (nm)**
35.5	0.010	14.6
38.7	0.009	16.3
48.8	0.012	12.1

3.3 Characterization of Coatings Using SEM

Figure 4 and Figure 5 illustrate how CuO and BPP are deposited on PANI coating, enhancing the corrosion inhibition efficiency by increasing the thickness of the inhibitor coating and the electron donating ability [44].

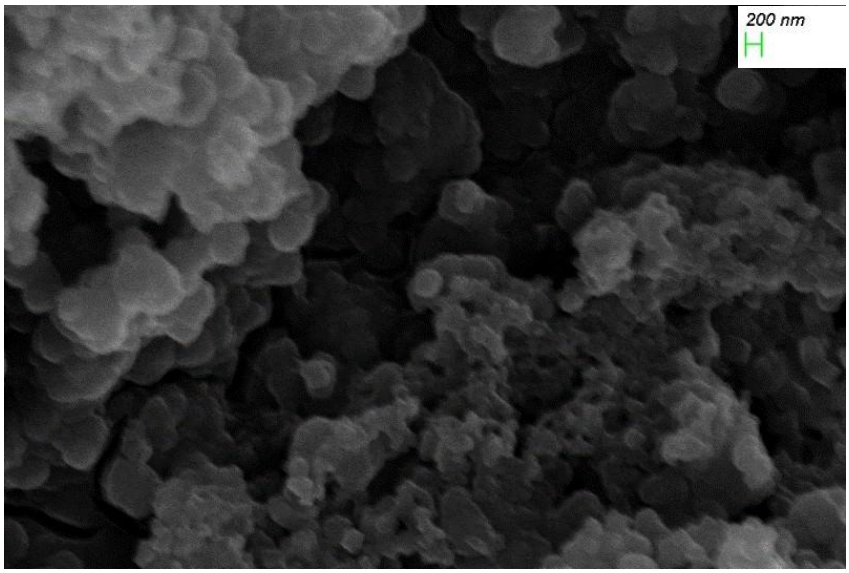


Figure 4: SEM of the coating made of polyaniline and banana peel powder extract

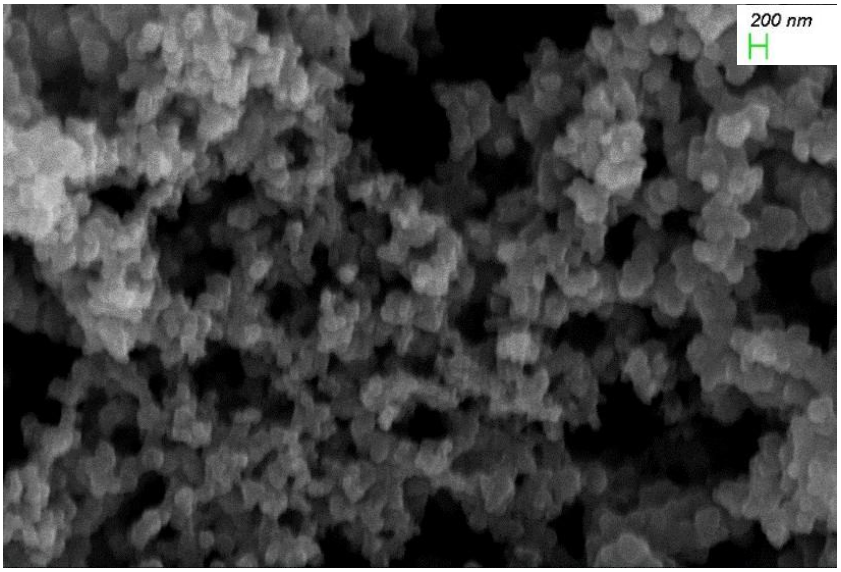
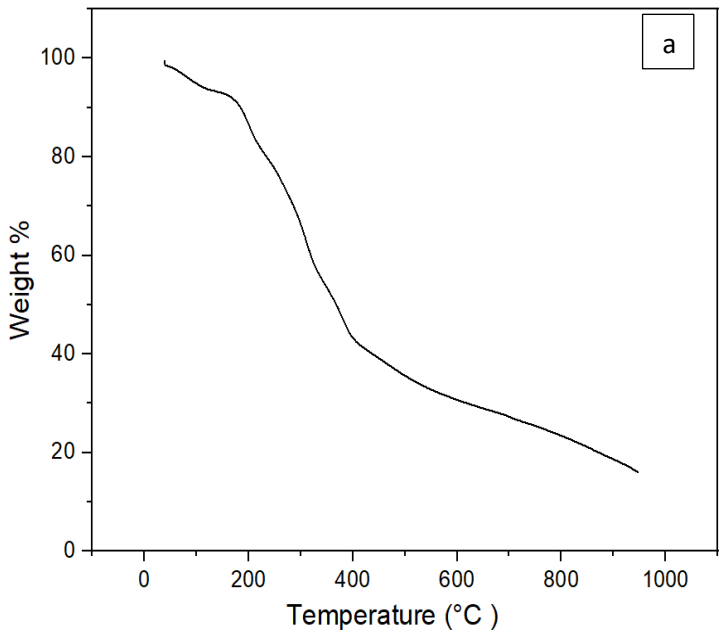


Figure 5: SEM of the coating made of polyaniline, CuO and banana peel powder extract

3.4 Thermogravimetric analysis (TGA)

Thermogravimetric analysis was conducted to evaluate the thermal stability of raw BPP, synthesized CuO, and carbonized BPP–CuO composite developed [44]. The TGA curves for each material are presented in Figure 6. Raw BPP exhibits significant mass loss due to its high organic content, together with moisture evaporation occurring at about 100 °C. The major decomposition of cellulose, hemicellulose and lignin occurs at 200–400 °C, and slow carbonization above 400 °C [45]. In contrast, CuO shows high thermal stability with only minor moisture loss below 150°C and no significant decomposition up to 800–900 °C, confirming its stable inorganic nature [46]. Carbonized BPP-CuO composite demonstrates improved thermal stability compared to that of raw BPP, with reduced mass loss and higher residual mass, due to the stabilizing effect of the CuO–carbon matrix [47]. The composite was specifically developed to enhance the long-term stability of BPP, making it more effective for sustained corrosion protection [48].



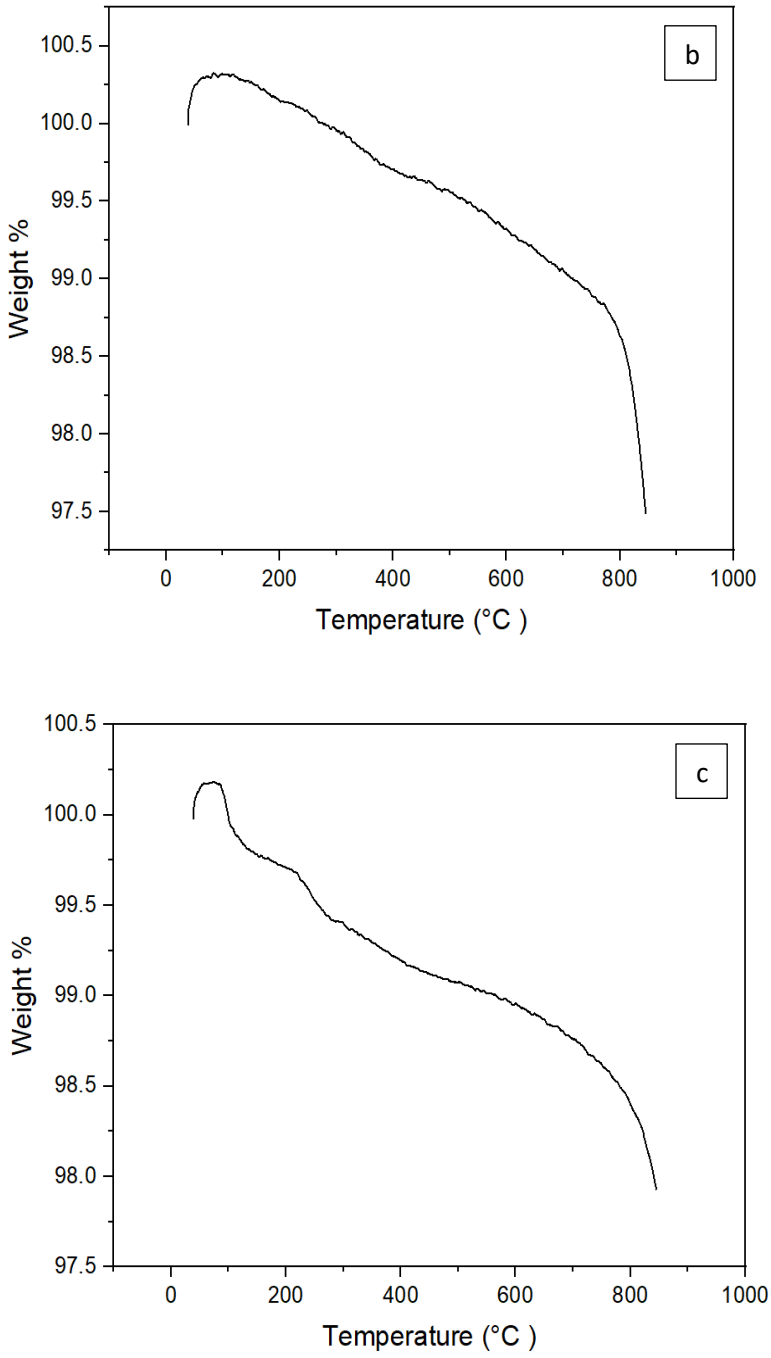


Figure 6: TGA curves of (a) raw BPP, (b) CuO and (c) carbonized BPP–CuO composite.

3.5 Investigation of Corrosion Inhibition Ability of Individual Inhibitors and Multi-Component Combined Layers

3.5.1 Mass loss memeasurements

Mass loss percentages shown in Figure 7 indicate that blank SS Grade 202 has the highest mass loss, while individual inhibitors such as BPP-, CuO- and PANI-coated SS Grade 202 have lower mass losses, indicating their corrosion inhibition ability [49,50]. Since corrosion rate and inhibition efficiency are inversely proportional, lower mass loss corresponds to higher corrosion protection [51]. Further, as the degree of dissolution depends on the surface area exposed and the time of exposure, SS Grade 202 specimens of similar sizes were used in all mass loss measurements [52]. Further, mass losses of all coated and uncoated specimens were recorded within similar exposure time intervals. Among the three inhibitors, PANI shows the best inhibitory activity as a single coating. Combination of BPP and CuO is better than individual coatings up to 4 days; nevertheless, PANI coatings are still better than individual BPP and CuO coatings, and their combination, indicating the necessity of PANI as a strong corrosion inhibitor. This is clearly demonstrated having much smaller mass losses associated with CuO+PANI, BPP+PANI coatings compared to individual and BPP+CuO coatings. More importantly, BPP+CuO+PANI coatings show the best corrosion inhibitory characteristics demonstrating the synergistic effect of the components.

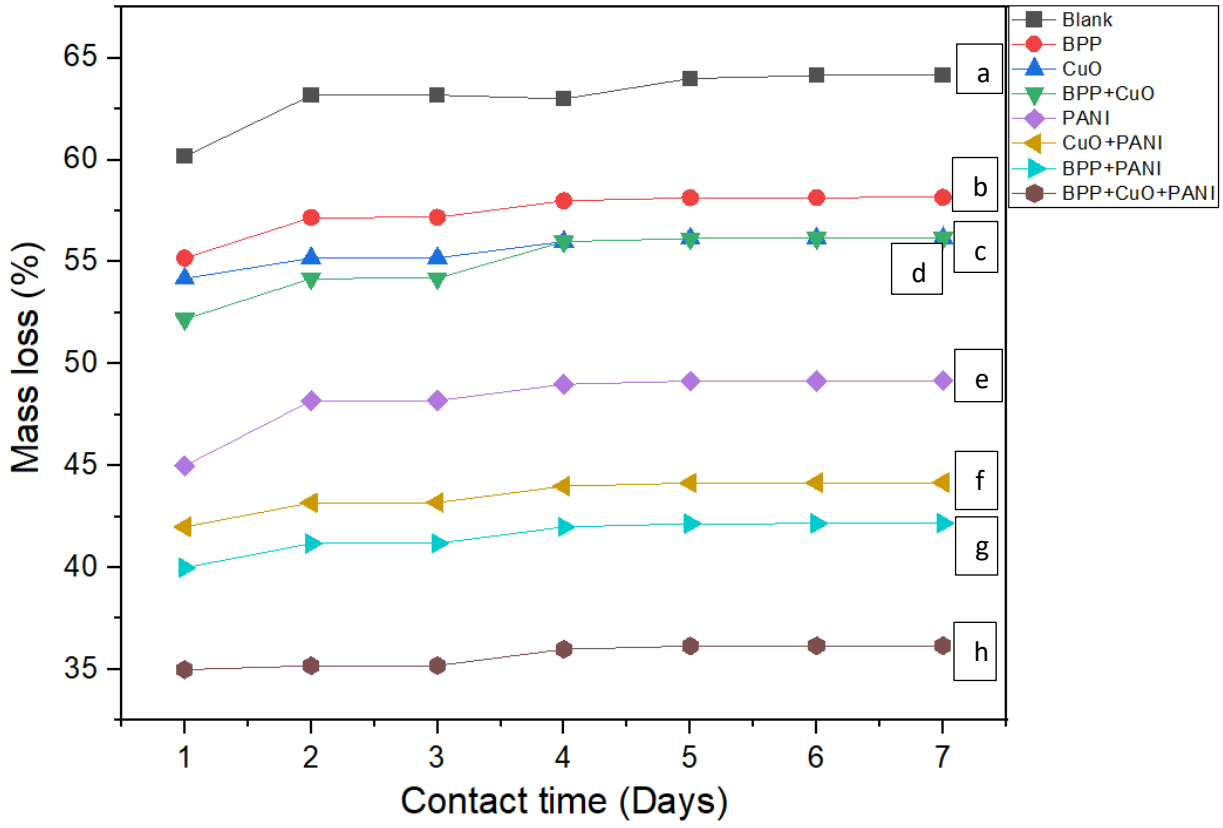


Figure 7: Mass loss of coated and uncoated SS Grade 202 specimens in 0.50 mol L^{-1} HCl (a) blank (b) BPP coated (c) CuO coated (d) PANI coated (e) BPP+CuO coated (f) CuO+PANI coated (g) BPP+PANI coated (h) BPP+CuO+PANI coated. Standard deviations (although not visible) are indicated as error bars.

3.5.2 Electrochemical impedance spectroscopy and equivalence circuits

Inhibitor-coated SS Grade 202 specimens show larger semicircle diameters compared to the blank specimen [53]. Since diameter of the semicircle is directly proportional to polarization resistance, blank SS Grade 202 has lower polarization resistance, while inhibitor-coated SS Grade 202 has higher values (Figure 8) [54]. Polarization resistance is inversely proportional to corrosion rate, indicating that blank SS Grade 202 has a higher corrosion rate, while coated samples have lower corrosion rates and greater inhibition [55]. PANI shows higher inhibition among the individual inhibitors [56]. Multi-component combined coatings further increase inhibition efficiency [57]. The BPP+CuO+PANI combination shows the best corrosion inhibition, supporting mass loss measurements, due to synergistic effect where the mixture

provides superior performance compared to individual components [58]. Polarization resistance values of each system investigated are given in Table 4 for comparison..

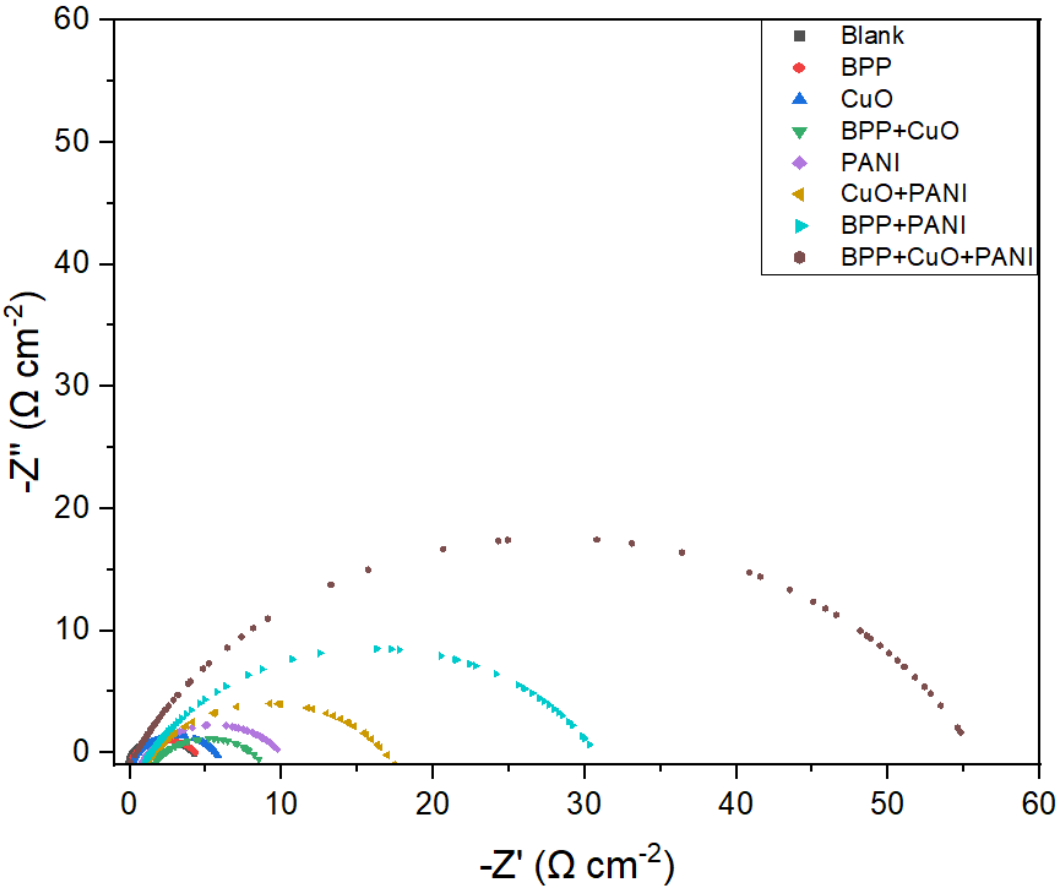


Figure 8: EIS spectra of of coated and uncoated SS Grade 202 specimens in 0.50 mol L^{-1} HCl (a) blank (b) BPP coated (c) CuO coated (d) PANI coated (e) BPP+CuO coated (f) CuO+PANI coated (g) BPP+PANI coated (h) BPP+CuO+PANI coated.

Table 4: Polarisation Resistance (R_p) Values of SS Grade 202 coated with individual inhibitors and combinations.

Solution / Inhibitor	R_p (Ω cm^{-2})
Blank	3.95
BPP	3.97
CuO	5.16
BPP+CuO	5.77
PANI	8.69
CuO+PANI	15.27
BPP+PANI	29.33
BPP+CuO+PANI	55.24

3.5.3 Tafel slope characteristics

Tafel slopes provide more accurate measurements than those produced by the mass loss method. Tafel slope determination is a vital electrochemical method in corrosion studies that correlates electrode potential and reaction rate of electrochemical systems, which are important to predict electron transfer pathways. Therefore, by identifying the anodic and cathodic Tafel slopes, corrosion potential and corrosion current which directly reflect the metal's corrosion rate can be deterrmined [59]. According to potentiodynamic polarization studies (Figure 9), the vertical axis corresponds to corrosion current density, where a higher current density implies a faster corrosion rate [60]. The horizontal axis represents the applied potential, the potential difference between the reference electrode, Ag/AgCl, and the working electrode, SS Grade 202. The inhibitors investigated act as mixed-type, reducing both anodic and cathodic reactions of SS Grade 202 in 0.50 mol L^{-1} HCl. Table 5 shows that adding the inhibitor significantly lowered the corrosion current density (Icorr), confirming its protective effect.

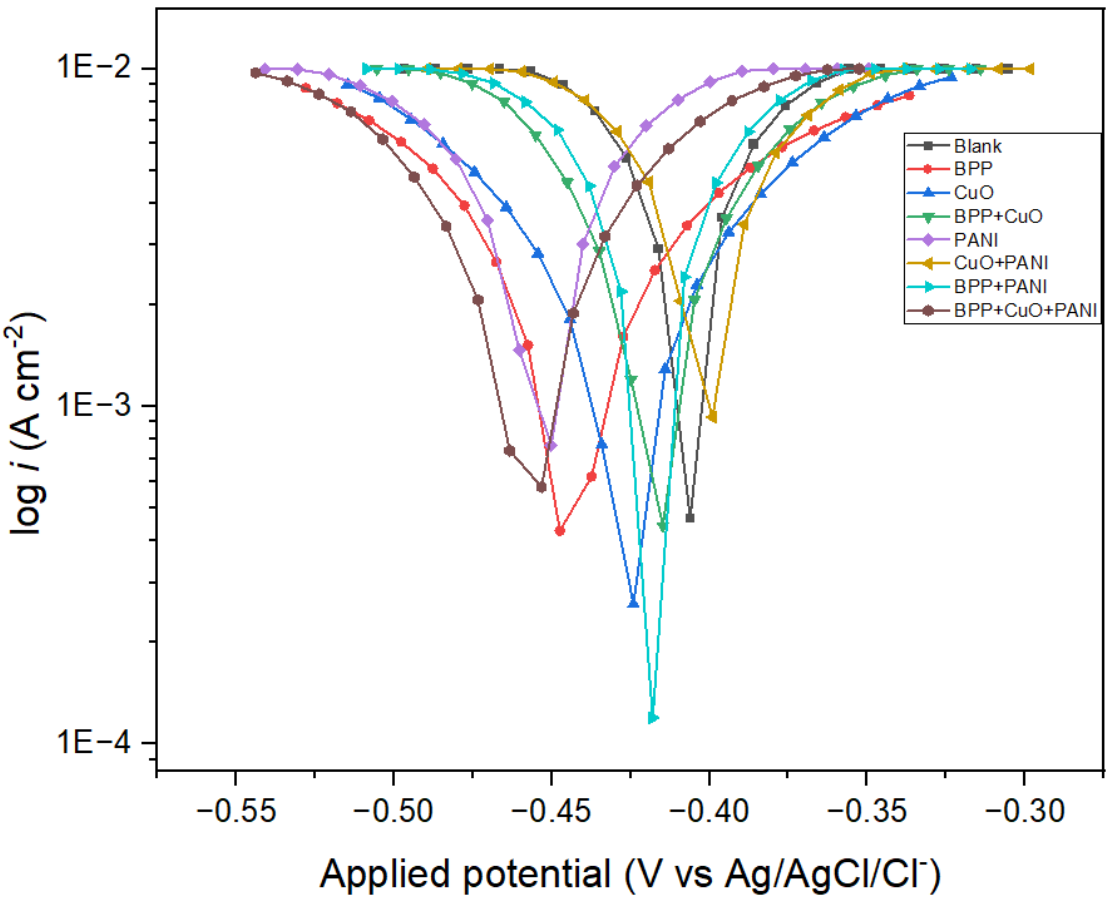


Figure 9: Tafel plots of coated and uncoated SS Grade 202 specimens in 0.50 mol L^{-1} HCl (a) blank (b) BPP coated (c) CuO coated (d) PANI coated (e) BPP+CuO coated (f) CuO+PANI coated (g) BPP+PANI coated (h) BPP+CuO+PANI coated.

Table 5: Tabulated values for corrosion potentials (E_{corr}), corrosion current (I_{corr}), and corrosion rate (mm year^{-1}) of SS Grade 202 coated with individual inhibitors and combinations.

Solution / Inhibitor	Corrosion potential (E_{corr})/ V ($\times 10^{-1}$)	Corrosion current (I_{corr})/A ($\times 10^{-3}$)	Corrosion rate/mm year^{-1}
Blank	-4.07	97.07	564.0
BPP	-4.43	33.83	196.5
CuO	-4.27	24.98	145.2
BPP + CuO	-4.18	24.32	141.3
PANI	-4.54	4.26	24.7
BPP + PANI	-4.02	3.80	22.1
CuO + PANI	-4.19	3.05	17.8
BPP + CuO + PANI	-4.58	2.25	13.1

Corrosion rates, with the corrosion potential corresponding to the minimum current, calculated from Tafel plots further confirm that inhibitor-coated specimens show significantly better corrosion protection than blank samples, with the PANI+CuO+BPP combined coating exhibiting the lowest corrosion current and corrposion rate.

3.5.4 Open circuit potential (OCP) measurements

The OCP profile of SS Grade 202 show an initial gradual increase over 100 min, indicating surface protection via inhibitor adsorption or passive layer formation (Figure 10). Fluctuations of OCP values, recorded between 100 min and 15 days, reflect dynamic surface interactions and localized corrosion. Stable OCP values obtained after 15 days indicate that a steady-state corrosion or passivation condition has reached. It is essential to measure the potential of the working electrodes up to a long period until the value becomes stable (Figure 11). Then only accurate and reliable trends of potential are acquired. Furthermore, this method is the most

appropriate for industrial applications as it requires only a multimeter/voltmeter, which is a portable instrument and a nondestructive method.

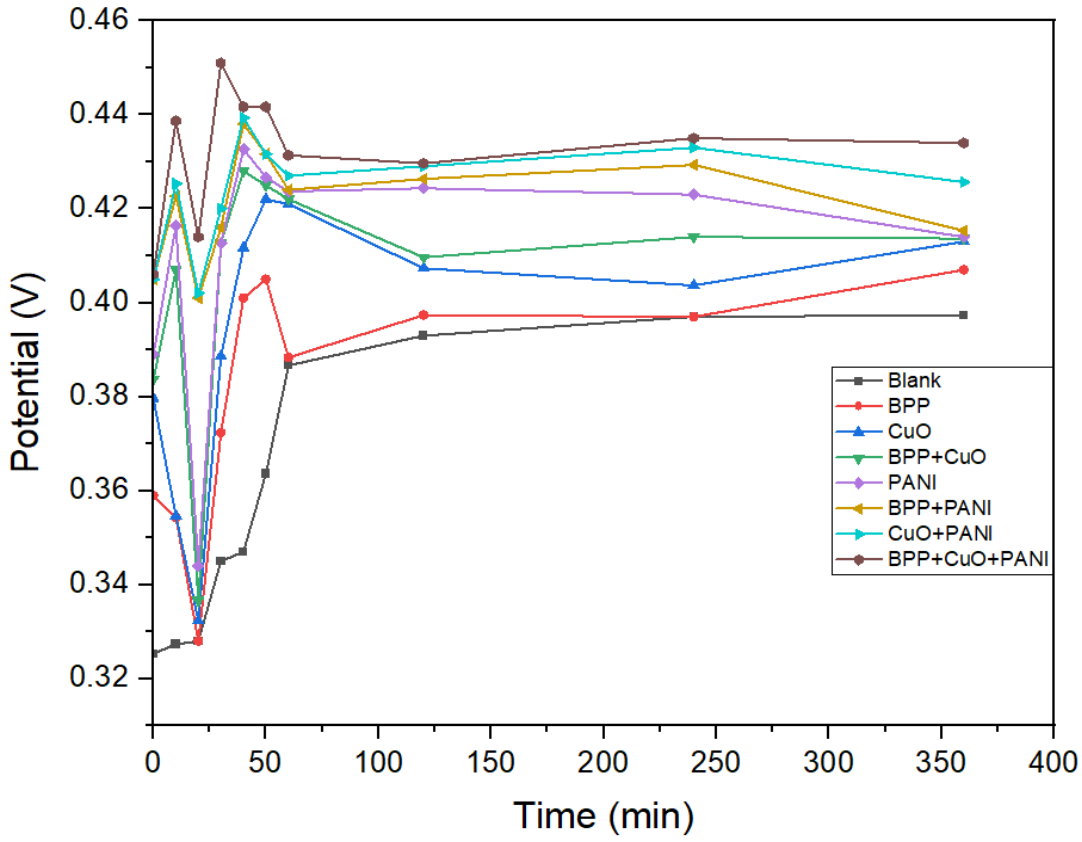


Figure 10: OCP values of coated and uncoated SS Grade 202 specimens in 0.50 mol L^{-1} HCl recorded within the first day (a) blank (b) BPP coated (c) CuO coated (d) PANI coated (e) BPP+CuO coated (f) CuO+PANI coated (g) BPP+PANI coated (h) BPP+CuO+PANI coated.

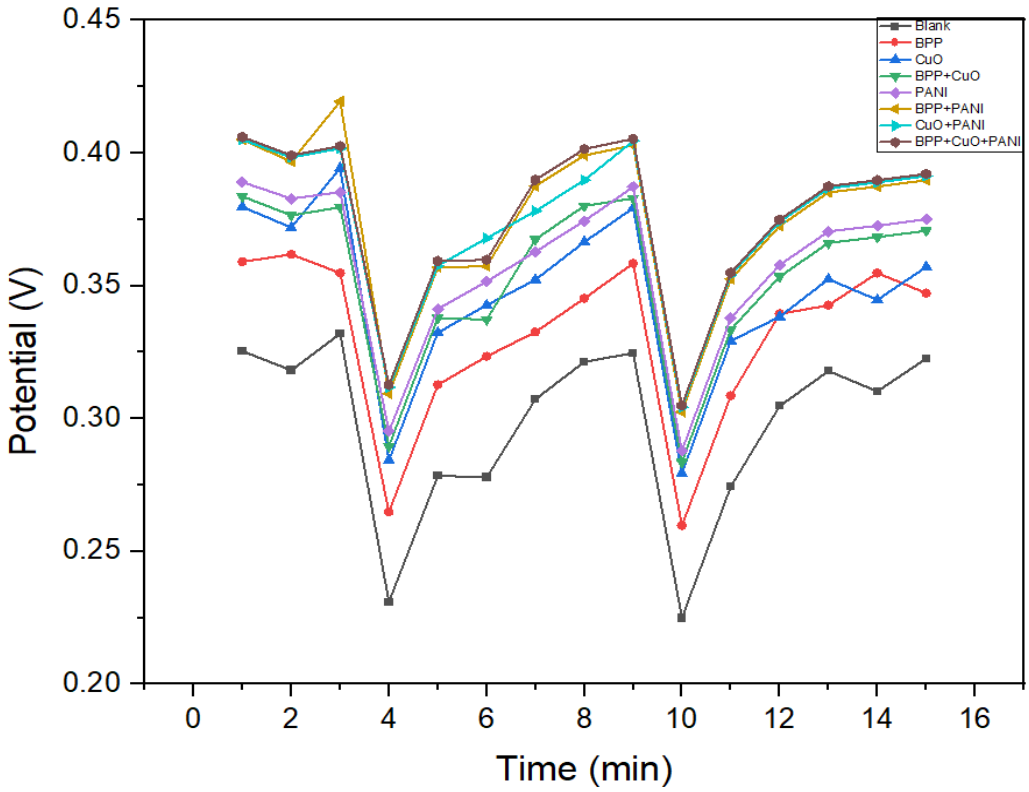


Figure 11: OCP values of coated and uncoated SS Grade 202 specimens in 0.50 mol L^{-1} HCl recorded over a 15-day period (a) blank (b) BPP coated (c) CuO coated (d) PANI coated (e) BPP+CuO coated (f) CuO+PANI coated (g) BPP+PANI coated (h) BPP+CuO+PANI coated.

4.Conclusion

Individual coatings of BPP, CuO and PANI demonstrate corrosion inhibitory characteristics on SS Grade 202 in the aggressive medium of 0.50 mol L^{-1} HCl, when compared to the blank system in the absence of any inhibitor. PANI, being the best corrosion inhibitor among the three corrosion inhibitors, provide stronger corrosion inhibitory action on SS Grade 202 when combined with BPP and CuO, as compared to relatively lower inhibitory action of BPP+CuO coatings. The combined coating of BPP+CuO+PANI demonstrates an extremely high corrosion inhibitory behavior due to synergistic effect of individual inhibitors as evidenced by a multi-technique approach of mass loss measurements, EIS, Tafel slope determinations and OCP measurements. The polarization resistance of the BPP+CuO+PANI coating on SS Grade 202 is improved by about 1300% with respect to the blank system further evidencing the superior

corrosion inhibition action of the three-component coating. Particles of CuO in the coating facilitate greater efficiency by enhancing surface coverage and forming a protective barrier layer. Green corrosion inhibitors such as BPP also exert high corrosion inhibition as they consist of bioactive compounds with high electron density, which could enhance the electron density of the SS Grade 202 substrate thereby inhibiting corrosion.

Acknowledgments

Special appreciation for the immense support provided by the Department of Environmental and Industrial Sciences and Department of Chemistry, Faculty of Science, University of Peradeniya, Sri Lanka.

Data Availability Statement

The data that supports this study will be shared upon reasonable request to the corresponding author; Namal Priyantha. (namal.priyantha@sci.pdn.ac.lk).

Conflicts of Interest

The authors declare that there are no conflicts of interest.

Declaration of Funding

This research did not receive any specific grant from funding agencies in the public, commercial, or not-for-profit sectors. Clinical trial number is not applicable.

Author Contributions

Author N. Priyantha contributed to the conceptualization of the study, funding acquisition, investigation and supervision. Data curation, data analysis, and writing the original draft of the manuscript were done by P.O.Alliyadde. Both authors contributed to reviewing and editing of the manuscript.

Consent for publication

All authors have given the consent for the publication of the manuscript and the materials incorporated.

Ethics approval

Not applicable. This research did not involve any human or animal subjects.

5.References

1. Abiola, O. K., Oforka, N. C., & Ebenso, E. E. (2007). Eco-friendly corrosion inhibitors: Inhibitive action of *Delonix regia* extract for the corrosion of aluminium in acidic medium. *Anti-Corrosion Methods and Materials*, 54(4), 219–224. https://doi.org/10.1108/00035590710762357
2. Akachukwu, N. D., Honesty, A. B., & John, A. (2024). Green corrosion inhibition: Utilizing banana pseudo-stem extract to protect mild steel in acidic environments. *Acta Chemica Malaysia*, 8(2), 66–80. https://doi.org/10.26480/acmy.02.2024.66.80
3. Akintelu, S. A., Folorunso, A. S., Folorunso, F. A., & Oyebamiji, A. K. (2020). Green synthesis, characterization and antimicrobial investigation of copper oxide nanoparticles synthesized using *Garcinia kola* leaf extract. *Nanomaterials*, 10(2), Article 217. https://doi.org/10.3390/nano10020217
4. Alhumaimess, M. S., Alshammari, H. M., Kamel, A. M., Hassan, H. M. A., & Mostafa, N. Y. (2021). Metal oxide nanoparticles as eco-friendly corrosion inhibitors for mild steel in 1.0 M HCl. *International Journal of Electrochemical Science*, 16(12), Article 211244. https://doi.org/10.20964/2021.12.38
5. Aljibori, H., Alamiery, A., & Kadhum, A. (2023). Advances in corrosion protection coatings: A comprehensive review. *International Journal of Corrosion and Scale Inhibition*, 12(4), 1450–1472. https://doi.org/10.17675/2305-6894-2023-12-4-6
6. Ambade, S., Tembhurkar, C., Rokde, A., Gupta, S., Shelare, S., Prakash, C., Gupta, L. R., & Smirnov, V. A. (2023). Experimental investigation of microstructural, mechanical and corrosion properties of 316L and 202 austenitic stainless steel joints using cold metal transfer welding. *Journal of Materials Research and Technology*, 27, 5881–5888. https://doi.org/10.1016/j.jmrt.2023.11.091
7. Ansari, K. R., Quraishi, M. A., & Singh, A. (2020). *Chromolaena odorata* leaf extract as a green corrosion inhibitor for mild steel in 1 M HCl: Experimental and theoretical studies. *Journal of Molecular Liquids*, 304, Article 112740. https://doi.org/10.1016/j.molliq.2020.112740
8. Ates, M., & Topala, T. (2014). Corrosion protection of polyaniline/CuO nanocomposite coatings on mild steel. *Corrosion Science*, 81, 311–321. https://doi.org/10.1016/j.corsci.2013.12.029
9. Bandeira, R. M., Lima, F. P., Nunes, M. S., Santos, E. C. D., Júnior, J. R. D. S., De Matos, J. M. E., Feitosa, C. M., Rai, M., Bhattarai, S., & Mulmi, D. D. (2025). The green plant-based corrosion inhibitors—a sustainable strategy for corrosion protection. *Surface Science and Technology*, 3(1), Article 84. https://doi.org/10.1007/s44251-025-00084-7
10. Bierwagen, G. P., & Tallman, D. E. (2001). Choice and evaluation of corrosion protective coatings. *Progress in Organic Coatings*, 41(1–3), 201–213. https://doi.org/10.1016/S0300-9440(01)00133-2
11. Chaudhari, S., & Patil, P. P. (2008). Corrosion protective bi-layered composites of polyaniline and poly(*o*-anisidine) on low carbon steel. *Journal of Applied Polymer Science*, 109(4), 2546–2561. https://doi.org/10.1002/app.28367
12. Chauhan, L. R., & Gunasekaran, G. (2007). Corrosion inhibition studies of plant extract in base oil. *Corrosion Science*, 49(3), 1143–1161. https://doi.org/10.1016/j.corsci.2006.06.014

13. Che, Z., Revilla, R. I., Li, C., Liu, J., Liu, W., Wouters, B., Marcoen, K., Cheng, X., Liu, C., & Li, X. (2024). Role of Te-RE alloying on the passive film and pitting corrosion behavior of 316L stainless steel. *Corrosion Science*, 240, Article 112457. https://doi.org/10.1016/j.corsci.2024.112457
14. Choudhary, S., Garg, A., & Mondal, K. (2016). Relation between open circuit potential and polarization resistance with rust and corrosion monitoring of mild steel. *Journal of Materials Engineering and Performance*, 25(7), 2969–2976. https://doi.org/10.1007/s11665-016-2112-6
15. Dalipi, R., Borgese, L., Casaroli, A., Boniardi, M., Fittschen, U., Tsuji, K., & Depero, L. (2015). Study of metal release from stainless steels in simulated food contact by means of total reflection X-ray fluorescence. *Journal of Food Engineering*, 173, 85–91. https://doi.org/10.1016/j.jfoodeng.2015.10.045
16. Ebenso, E. E., Kabanda, M. M., & Murulana, L. C. (2021). Quantum chemical calculations and Monte Carlo simulations on plant extracts as eco-friendly corrosion inhibitors. *Journal of Molecular Structure*, 1225, Article 129188. https://doi.org/10.1016/j.molstruc.2020.129188
17. El-Etre, A. Y. (2003). Inhibition of acid corrosion of carbon steel using natural honey. *Corrosion Science*, 45(11), 2485–2495. https://doi.org/10.1016/S0010-938X(03)00066-0
18. El-Lateef, H. M. A., Khalaf, M. M., & Gouda, M. (2020). Assessment of corrosion coupon monitoring and inhibition in oilfield water injection systems. *Journal of Petroleum Science and Engineering*, 195, Article 107623. https://doi.org/10.1016/j.petrol.2020.107623
19. El-Sayed, A., Mohran, H. S., & El-Lateef, H. M. A. (2011). Corrosion study of zinc, nickel, and zinc-nickel alloys in alkaline solutions by Tafel plot and impedance techniques. *Metallurgical and Materials Transactions A*, 43(2), 619–632. https://doi.org/10.1007/s11661-011-0908-4
20. Fatahiamirdehi, M., Mahani, M., Mirseyed, S. F., Rostamian, A., & Ostadhassan, M. (2024). Enhancing corrosion resistance of 316L stainless steel through electrochemical deposition of polyaniline coatings in acidic environments. *Journal of Materials Science*, 59(31), 14716–14727. https://doi.org/10.1007/s10853-024-10047-2
21. Finšgar, M., & Jackson, J. (2014). Application of corrosion inhibitors in oil and gas production: A review. *Corrosion Science*, 86, 17–41. https://doi.org/10.1016/j.corsci.2014.04.044
22. Fiori, F., Marchesi, S., & Rossi, L. (2021). Plant-derived bio-extracts as sustainable corrosion inhibitors: Mechanism and industrial viability. *Industrial & Engineering Chemistry Research*, 60(14), 5120–5132. https://doi.org/10.1021/acs.iecr.1c00245
23. Flitt, H. J., & Schweinsberg, D. P. (2005). Evaluation of corrosion rate from polarisation curves not exhibiting a Tafel region. *Corrosion Science*, 47(12), 3034–3052. https://doi.org/10.1016/j.corsci.2005.06.014
24. Geniès, E. M., Boyle, A., Lapkowski, M., & Tsintavis, C. (1990). Polyaniline: A historical survey. *Synthetic Metals*, 36(2), 139–182. https://doi.org/10.1016/0379-6779(90)90050-U
25. Gudić, S., Nagode, A., Šimić, K., Vrsalović, L., & Jozić, S. (2022). Corrosion behavior of different types of stainless steel in PBS solution. *Sustainability*, 14(14), Article 8935. https://doi.org/10.3390/su14148935

26. Gunavathy, N., & Murugavel, S. C. (2013). Corrosion inhibition of mild steel in acid media by *Musa acuminata* peel extract. *Journal of Chemistry*, 2013, Article 824317. https://doi.org/10.1155/2013/824317
27. Haldhar, R., Prasad, D., & Saxena, A. (2020). *Myristica fragrans* extract as an eco-friendly corrosion inhibitor for mild steel in acidic medium: Experimental and theoretical studies. *Sustainable Chemistry and Pharmacy*, 15, Article 100209. https://doi.org/10.1016/j.scp.2019.100209
28. Hidalgo, D., Montero, C., Luna, D., Pazmiño, V., & Brito, J. (2025). Evaluation of banana-derived inhibitor for corrosion control in mild steel. *Civil Engineering and Architecture*, 13(1), 664–677. https://doi.org/10.13189/cea.2025.130142
29. Ismail, A., & Tajuddin, M. A. M. (2016). Eco-friendly banana peel extract as corrosion inhibitor for stainless steel in aggressive aqueous media. *Journal of Bio- and Tribo-Corrosion*, 2(4), Article 24. https://doi.org/10.1007/s40735-016-0054-9
30. Jamaluddin, J. B., Paramitha, T., Salsabila, I. N., Luviana, A., Ramadhan, M. Z., Putri, A., Nurbaits, A., & Sihombing, R. P. (2024). Characterization of banana peel corrosion inhibitor by vacuum microwave assisted extraction (VMAE) method in 2% HCl environment. *International Journal of Applied Technology Research*, 5(1), 1–10. https://doi.org/10.35313/ijatr.v5i1.144
31. Javaherdashti, R. (2000). How corrosion affects industry and life. *Anti-Corrosion Methods and Materials*, 47(1), 30–34. https://doi.org/10.1108/00035590010309730
32. Jegdić, B., Dražić, D. M., & Popić, J. P. (2008). Open circuit potentials of metallic chromium and austenitic 304 stainless steel in aqueous sulphuric acid solution and the influence of chloride ions on them. *Corrosion Science*, 50(5), 1235–1244. https://doi.org/10.1016/j.corsci.2008.01.012
33. Ji, G., Anjum, S., Sundaram, S., & Prakash, R. (2015). Eco-friendly plant extracts as corrosion inhibitors of mild steel in hydrochloric acid medium. *Corrosion Science*, 90, 107–117. https://doi.org/10.1016/j.corsci.2014.10.002
34. Kaur, J., Daksh, N., & Saxena, A. (2021). Corrosion inhibition applications of natural and eco-friendly corrosion inhibitors on steel in the acidic environment: An overview. *Arabian Journal for Science and Engineering*, 47(1), 57–74. https://doi.org/10.1007/s13369-021-05699-0
35. Khan, M. A. A., Irfan, O. M., Djavanroodi, F., & Asad, M. (2022). Development of sustainable inhibitors for corrosion control. *Sustainability*, 14(15), Article 9502. https://doi.org/10.3390/su14159502
36. Lai, X. B., Dao, T.-B.-N., Duong-Ngo, K.-L., Tran, T. N., Le Minh, T., Nguyen Trong, H., Hoang Ngoc, C. T., Panaitescu, C., To Hoai, N., & Dang, N. N. (2023). Inhibitive behaviours of unripe banana peel extract for mitigating electrochemical corrosion of carbon steel in aggressively acidic solutions. *Journal of Taibah University for Science*, 17(1), Article 2247633. https://doi.org/10.1080/16583655.2023.2247633
37. Lazanas, A. C., & Prodromidis, M. I. (2023). Electrochemical impedance spectroscopy—A tutorial. *ACS Measurement Science Au*, 3(3), 162–193. https://doi.org/10.1021/acsmeasuresciau.2c00070
38. Li, K., Sun, L., Cao, W., Chen, S., Chen, Z., Wang, Y., & Li, W. (2022). Pitting corrosion of 304 stainless steel in secondary water supply system. *Corrosion Communications*, 7, 43–50. https://doi.org/10.1016/j.corcom.2021.11.010

39. Lu, W.-K., Elsenbaumer, R. L., & Wnek, G. E. (1995). Corrosion protection with conducting polymers: Polyaniline coatings on cold rolled steel. *Synthetic Metals*, 71(1–3), 2163–2166. https://doi.org/10.1016/0379-6779(94)03204-Q
40. Malaret, F. (2022). Exact calculation of corrosion rates by the weight-loss method. *Experimental Results*, 3, Article e5. https://doi.org/10.1017/exp.2022.5
41. Manikandan, C. B., Saranya, R., & Rajaram, N. (2019). Corrosion inhibition of mild steel by using banana peel extract. *International Journal of Modern Trends in Engineering and Research*, 6(4), 11–17. https://doi.org/10.21884/IJMTER.2019.6083
42. Muralidharan, S., Saraswathy, V., & Thangavel, K. (2022). Electrochemical performance of bio-based nano-composite coatings for severe atmospheric exposure. *Surface and Coatings Technology*, 434, Article 128190. https://doi.org/10.1016/j.surfcoat.2022.128190
43. Nwosu, F. O., Osarolube, E., & Okewale, A. O. (2020). Corrosion inhibition of low-carbon steel in acidic media using agricultural waste extracts. *Journal of Failure Analysis and Prevention*, 20(4), 1342–1352. https://doi.org/10.1007/s11668-020-00942-1
44. Pan, B., Qian, K., Xie, H., & Asundi, A. (2009). Two-dimensional digital image correlation for in-plane displacement and strain measurement: A review. *Measurement Science and Technology*, 20(6), Article 062001. https://doi.org/10.1088/0957-0233/20/6/062001
45. Panchal, J., Shah, D., Patel, R., Shah, S., Prajapati, M., & Shah, M. (2021). Comprehensive review and critical data analysis on corrosion and emphasizing on green eco-friendly corrosion inhibitors for oil and gas industries. *Journal of Bio- and Tribo-Corrosion*, 7(3), Article 107. https://doi.org/10.1007/s40735-021-00540-5
46. Parangusan, H., Sliem, M. H., Abdullah, A. M., Elhaddad, M., Al-Thani, N., & Bhadra, J. (2024). Plant extract as green corrosion inhibitors for carbon steel substrate in different environments: A systematic review. *International Journal of Electrochemical Science*, 20(4), Article 100919. https://doi.org/10.1016/j.ijoes.2024.100919
47. Popoola, L. T. (2019). Progress on pharmaceutical drugs, plant extracts and ionic liquids as corrosion inhibitors. *Heliyon*, 5(2), Article e01143. https://doi.org/10.1016/j.heliyon.2019.e01143
48. Ramezanzadeh, B., Ahmadi, A., & Mahdavian, M. (2016). Enhancement of the corrosion protection performance of an epoxy coating decorated with surface-modified copper oxide (CuO) nanoparticles. *Journal of the Taiwan Institute of Chemical Engineers*, 68, 440–454. https://doi.org/10.1016/j.jtice.2016.09.029
49. Reddy, K. C. P., Ramesh, S., & Reddy, P. S. (2020). Banana peel powder corrosion inhibition of mild steel in acid medium. *Journal of Bio- and Tribo-Corrosion*, 6(4), Article 94. https://doi.org/10.1007/s40735-020-00392-4
50. Priyantha, N., Jayasingha, J. M. S., & Wijesooriya, W. M. G. S. (2021). Inhibitive action of selected model compounds of eugenol on mild steel corrosion in salty medium. *Protection of Metals and Physical Chemistry of Surfaces*, 57(2), 412–421. https://doi.org/10.1134/s2070205121010159
51. Revon, M. H. N., & Priyantha, N. (2025). Interference of solution constituents on corrosion inhibition of phosphate species on Grade 202 stainless steel. *Discover Chemistry*, 2(1), Article 125. https://doi.org/10.1007/s44371-025-00157-4
52. Revon, M. H. N., & Priyantha, N. (2026). Superior corrosion inhibition activity of CaO nanoparticles synthesized from natural sources toward stainless-steel Grade 202 in

chloride-rich media. *Discover Electrochemistry*, 3(1), Article 23. https://doi.org/10.1007/s44293-026-00023-x

53. Rosli, N. R., Mat Yusuf, S., Sauki, A., & Wan Razali, W. M. R. (2019). *Musa sapientum* (banana) peels as green corrosion inhibitor for mild steel. *Key Engineering Materials*, 797, 230–239. https://doi.org/10.4028/www.scientific.net/KEM.797.230
54. Sangeetha, M., Rajendran, S., & Sathiyabama, J. (2021). Eco-friendly hydrophobic nano-thin films from banana peel extract for corrosion protection of steel in marine environments. *Journal of Molecular Liquids*, 335, Article 116370. https://doi.org/10.1016/j.molliq.2021.116370
55. Sangeetha, M., Rajendran, S., Sathiyabama, J., & Prabhakar, P. (2013). Eco-friendly extract of banana peel as corrosion inhibitor for carbon steel in seawater. *Journal of Materials and Environmental Science*, 4(5), 601–610.
56. Senthooran, R., Revon, M. H. N., & Priyantha, N. (2025). Cinnamon leaf extract as an effective inhibitor for mild steel corrosion in pickling bath environments. *Discover Chemistry*, 2(1), Article 83. https://doi.org/10.1007/s44371-025-00083-5
57. Shao, Z., Yu, D., Shao, D., Du, Y., Zheng, D., Qiu, Z., & Wu, B. (2023). A protective role of Cl^- ion in corrosion of stainless steel. *Corrosion Science*, 226, Article 111631. https://doi.org/10.1016/j.corsci.2023.111631
58. Tuken, T., Yagan, A., & Yazici, B. (2007). Polyaniline coatings electropolymerization on mild steel. *Progress in Organic Coatings*, 59(3), 297–303. https://doi.org/10.1016/j.porgcoat.2007.01.016
59. Van Der Heijden, O., Park, S., Vos, R. E., Eggebeen, J. J. J., & Koper, M. T. M. (2024). Tafel slope plot as a tool to analyze electrocatalytic reactions. *ACS Energy Letters*, 9(4), 1871–1879. https://doi.org/10.1021/acsenergylett.4c00266
60. Zhao, R., Yu, Q., & Niu, L. (2021). Corrosion inhibition of amino acids for 316L stainless steel and synergistic effect of I^- ions: Experimental and theoretical studies. *Materials and Corrosion*, 73(1), 31–44. https://doi.org/10.1002/maco.202112511

Supplementary Files

This is a list of supplementary files associated with this preprint. Click to download.

- GraphicalAbstrct.pdf